POLITECNICO DI TORINO
Repository ISTITUZIONALE

Invisibility utilizing Huygens' metasurface based on mantle cloak and scattering suppression phenomen

(Article begins on next page)

18 October 2022

Communication

Invisibility Utilizing Huygens' Metasurface based on Mantle Cloak and Scattering Suppression Phenomena

Hemn Younesiraad, Zahra Hamzavi-Zarghani, and Ladislau Matekovits, *Senior Member, IEEE*

Abstract—This paper presents the design of a Huygens' metasurface (HMS) coating aiming to achieve strongly enhanced invisibility. An analytical formulation for obtaining the required electric surface admittance and magnetic surface impedance is presented. The proposed unit cell consists of a pair of split-rin resonators in the top layer and a metal capacitor in the bottom layer of the same substrate. The geometries are properly designed to provide the required electric surface admittance and magnetic surface impedance for maximum scattering reduction at the operational frequency of 4 GHz. The designed HMS is optimized to realize the required electric surface admittance and magnetic surface impedance for remarkable cloaking purposes. Scattering-cross section (SCS) of uncloaked and cloaked conducting cylinders is obtained with CST Microwave Studio simulation which matches the analytical results. The results show robust scattering reduction with considerable bandwidth for the covered cylinder by the HMS. Furthermore, the obtained results with HMS are compared with the results presented in the literature for cloaking with ordinary metasurface. This comparison emphasizes a much better cloaking performance of the HMS. Considerable cloaking obtained in this paper can be applied for invisibility purposes, sensing applications, antenna isolation, radiation blockage reduction in antennas, eta.

Index Terms—Huygens' Metasurface, Invisibility, Mantle Cloaking, Radar Cross Section, Scattering.

I. INTRODUCTION

IN recent years, the electromagnetic cloak has been one of the essential and exciting topics for researchers, leading to a variety of intriguing phenomena and applications such as invisibility [1], nonintrusive sensing [2], and communications [3]. To accomplish these features, one can manipulate the reflected and transmitted waves due to an incident wave onto an object using electromagnetic (EM) theory and utilizing new artificial materials to make the object appear invisible. One of the innovative ways to achieve EM cloak is to use metamaterials so that they can reduce or control the scattering waves spanning from radio-frequency (RF) to optical regimes [4]-[10]. Some of the EM cloak approaches are transformation optics [11], carpet cloak based on quasi-conformal mapping [12]-[13], and transmission line cloaking [14]. The transformation optics technique is based on inhomogeneous

and anisotropic metamaterials which can bend EM waves around the object without any reflection, leading to effective invisibility in the near-infrared and visible range of frequencies [11]. In addition to the cloaking methods mentioned above, plasmonic cloaking [15] and mantle cloaking [16]-[18] techniques can be considered in which metasurfaces are used instead of bulk metamaterial, which overcomes predictable difficulties such as the fabrication difficulties, high dispersion and loss of metamaterials due to their resonance feature. Creative use of metasurfaces due to their unique properties and potential ability in manipulating EM waves can be a very good alternative. In plasmonic cloaking utilizing metamaterials lead to the anti-phase scattered field property, the majority of the scattered fields can be canceled which results in the invisibility of a given object. The mantle cloak approach is based on the cancellation of extreme scattered waves by adjusting the parameters of the metasurface wrapping around a given object without using bulk metamaterials, which can be realized with stable technology utilizing metasurfaces for practical realization and robust performance. Some extensions of the research in the mantle cloak based on scattering suppression include anisotropic metasurface cloak [19], tunable metasurface cloak [20], metasurface cloak for dual-polarized plane waves [21], wide-band metasurface cloak [22], dual-band mantle cloak [23], and multilayer mantle cloak [24]. In these researches, a simple method has been applied to design the metasurface which provides only electric polarized current to generate prescribed wavefronts. Alternatively, Huygens' metasurface (HMS) based on Huygens' principle can manipulate the transmission and reflection of the waves, independently. HMS has offered a robust approach to the ultimate control of EM fields by generating orthogonal equivalent electric and magnetic currents to control the scattered waves for specific EM interaction exquisitely [25]-[26]. Using this approach, a better ability to manipulate the phase, amplitude, and polarization of EM waves can be obtained, compared to only adjusting electric surface impedance. Due to the strong wave-manipulating ability of HMS, unique contributions have been reported in high-efficiency generation of airy beams [27], polarization controlling devices [28], and perfect absorbers [29]. It is shown in [30], that utilizing Huygen's principle to superimpose magnetic and electric surface current densities that can be discretized into electric and magnetic dipoles at the boundary of an object, leads to an improved cloak for EM waves.

H. Younesiraad is with the Department of Electrical and Computer Engineering, University of Tabriz, Tabriz, Iran, and the Department of Electrical Engineering, University of Kurdistan, Sanandaj, Iran (e-mail: younesiraad@tabrizu.ac.ir).

Z. Hamzavi-Zarghani is with the Dipartimento di Elettronica e Telecomunicazioni, Politecnico di Torino, Torino, 10129, Italy.

L. Matekovits is with the Department of Electronics and Telecommunications, Politecnico di Torino, Turin, Italy, Istituto di Elettronica e di Ingegneria dell'Informazione e delle Telecomunicazioni, National Research Council of Italy, 10129 Turin, Italy, and Politehnica University Timisoara, Romania.

II. THEORY

Figure 1 shows the geometry of the solvable problem in which an infinite perfect electric conductor (PEC) with radius b is covered by a thin HMS layer with radius a. The space between the conductor and the HMS layer is filled by a dielectric spacer with a relative permittivity ϵ_r. The structure illustrated in Fig. 1 is illuminated by a normally incident TM-polarized plane wave of amplitude E_0. The EM field expressions in each region can be written as [24]:

$$\mathbf{E}^{(1)} = \hat{\mathbf{z}} E_0 \sum_n j^{-n} e^{jn\phi} \big(A_n J_n(k_d \rho) + B_n Y_n(k_d \rho) \big) \quad (1)$$

$$\mathbf{H}^{(1)} = \hat{\boldsymbol{\phi}} \frac{E_0}{j\eta_d} \sum_n j^{-n} e^{jn\phi} \big(A_n J_n'(k_d \rho) + B_n Y_n'(k_d \rho) \big) \quad (2)$$

for $b < \rho < a$, and

$$\mathbf{E}^{(2)} = \hat{\mathbf{z}} E_0 \sum_n j^{-n} e^{jn\phi} \big(J_n(k_0 \rho) + R_n H_n^{(2)}(k_0 \rho) \big) \quad (3)$$

$$\mathbf{H}^{(2)} = \hat{\boldsymbol{\phi}} \frac{E_0}{j\eta_0} \sum_n j^{-n} e^{jn\phi} \big(J_n'(k_0 \rho) + R_n H_n^{(2)\prime}(k_0 \rho) \big) \quad (4)$$

for $\rho > a$, where $J_n(\cdot)$ and $Y_n(\cdot)$ are Bessel functions of the first and second kind of order n. The Hankel function is represented as $H_n^{(2)}(\cdot) = J_n(\cdot) - jY_n(\cdot)$. η_0 and k_0, are the intrinsic impedance and wavenumber of the free space, respectively, and $\eta_d = \eta_0 / \sqrt{\epsilon_{\text{eff}}}$. The prime on Bessel, Neuman and Hankel functions refers to the first order partial derivative with respect to their arguments. The boundary conditions governing the HMS and PEC interfaces in terms of EM fields and fictitious electric and magnetic surface currents can be used to calculate the unknown coefficients A_n, B_n and R_n at $\rho = a, b$. Based on the surface equivalence principle, the boundary condition can be expressed as

$$\overline{\overline{Y}}_{es} \cdot E_{T,ave} = \hat{\boldsymbol{\rho}} \times (\mathbf{H}^{(2)} - \mathbf{H}^{(1)}) \quad (5)$$

$$\overline{\overline{Z}}_{ms} \cdot H_{T,ave} = -\hat{\boldsymbol{\rho}} \times (\mathbf{E}^{(2)} - \mathbf{E}^{(1)}) \quad (6)$$

where subscript of (1) and (2) refer to the spacer and the free space regions, respectively as well as $\overline{\overline{Y}}_{es}$, and $\overline{\overline{Z}}_{ms}$ are

dyadic electric sheet admittance and dyadic magnetic sheet impedance defined as

$$\overline{\overline{Y}}_{es} = j\omega \overline{\overline{\alpha}}_{ee}^{\text{eff}} \quad (7)$$

$$\overline{\overline{Z}}_{ms} = j\omega \overline{\overline{\alpha}}_{mm}^{\text{eff}} \quad (8)$$

where $\overline{\overline{\alpha}}_{ee}^{\text{eff}}$ and $\overline{\overline{\alpha}}_{mm}^{\text{eff}}$ are effective electric and magnetic polarizabilities of constituent particles formed the HMS. The expressions $E_{T,ave}$ and $H_{T,ave}$ represent the average tangential electric and magnetic fields at $\rho = a$. The other required boundary condition at PEC interface reads as

$$\mathbf{E}^{(1)} \times \hat{\boldsymbol{\rho}} = 0 \quad (9)$$

Substituting the EM fields expressed in Eqs. (1)-(4) in (5), (6), and (9), thus solving the obtained equations by using Cramer's rule, the scattering coefficient of the nth mode is given by Eq. (10). For EM wave scattering suppression corresponding to cloaking, the reflection coefficient should be equal to zero for each mode. Since the absorptivity of the HMS is negligible, so Y_{es} and Z_{ms} are pure imaginary values. To calculate the unknown coefficients and according to the initial assumption that the radius of the cylinder is considered to be very small relative to the wavelength, we consider a convenient assumption as $|R_n|^2 + |A_n|^2 + |B_n|^2 = 1$.
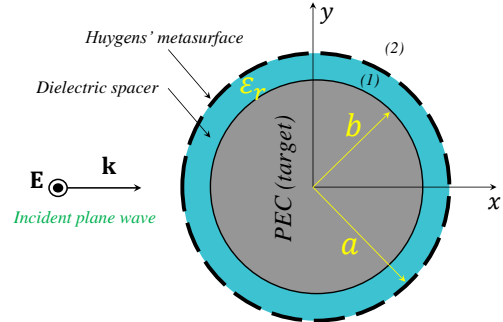

Fig. 1: Schematic geometry of a PEC cylinder and dielectric spacer covered by a conformal HMS, illuminated by a normally incident TM-polarized plane wave.

$$R_n = \frac{\begin{vmatrix} -J_n'(k_0 a) + \frac{j\eta_0 Y_{es}}{2} J_n(k_0 a) & -\frac{j\eta_0 Y_{es}}{2} J_n(k_d a) - \sqrt{\epsilon_{\text{eff}}} J_n'(k_d a) & -\frac{j\eta_0 Y_{es}}{2} Y_n(k_d a) - \sqrt{\epsilon_{\text{eff}}} Y_n'(k_d a) \\ -J_n(k_0 a) + \frac{Z_{ms}}{2j\eta_0} J_n'(k_0 a) & -\frac{Z_{ms}}{2j\eta_0} \sqrt{\epsilon_{\text{eff}}} J_n'(k_d a) - J_n(k_d a) & -\frac{Z_{ms}}{2j\eta_0} \sqrt{\epsilon_{\text{eff}}} Y_n'(k_d a) - Y_n(k_d a) \\ 0 & J_n(k_d b) & Y_n(k_d b) \end{vmatrix}}{\begin{vmatrix} -\frac{j\eta_0 Y_{es}}{2} H_n^{(2)}(k_0 a) + H_n^{(2)\prime}(k_0 a) & -\frac{j\eta_0 Y_{es}}{2} J_n(k_d a) - \sqrt{\epsilon_{\text{eff}}} J_n'(k_d a) & -\frac{j\eta_0 Y_{es}}{2} Y_n(k_d a) - \sqrt{\epsilon_{\text{eff}}} Y_n'(k_d a) \\ -\frac{Z_{ms}}{2j\eta_0} H_n^{(2)\prime}(k_0 a) + H_n^{(2)}(k_0 a) & -\frac{Z_{ms}}{2j\eta_0} \sqrt{\epsilon_{\text{eff}}} J_n'(k_d a) - J_n(k_d a) & -\frac{Z_{ms}}{2j\eta_0} \sqrt{\epsilon_{\text{eff}}} Y_n'(k_d a) - Y_n(k_d a) \\ 0 & J_n(k_d b) & Y_n(k_d b) \end{vmatrix}} \quad (10)$$

$$\frac{j\eta_0 Y_{es}}{2} = -\frac{\pm M \sqrt{\epsilon_{\text{eff}}} \big(J_n'(k_d a) Y_n(k_d b) - J_n(k_d b) Y_n'(k_d a) \big) - Y_n(k_d b) J_n'(k_0 a)}{\pm M \big(J_n(k_d a) Y_n(k_d b) - J_n(k_d b) Y_n(k_d a) \big) + Y_n(k_d b) J_n(k_0 a)} \quad (11)$$

$$\frac{Z_{ms}}{2j\eta_0} = -\frac{\pm M \big(J_n(k_d a) Y_n(k_d b) - J_n(k_d b) Y_n(k_d a) \big) - Y_n(k_d b) J_n(k_0 a)}{\pm M \sqrt{\epsilon_{\text{eff}}} \big(J_n'(k_d a) Y_n(k_d b) - J_n(k_d b) Y_n'(k_d a) \big) + Y_n(k_d b) J_n'(k_0 a)} \quad (12)$$

Using this relation and the boundary conditions given in Eqs. (5), (6), and (9), the desired electric sheet admittance and magnetic sheet impedance expressions to achieve invisibility can be found as equations (11) and (12), where

$$M = \frac{1}{\left|\frac{J_n(k_d b)}{Y_n(k_d b)}\right|^2 + 1} \tag{13}$$

Based on the approximate expressions of the small argument of the first-order Bessel functions when the radius of the cylinder is very small relative to the wavelength, then the $M \cong 1$, which is consistent with the claim of $A_n \cong 1$ and $B_n \cong 0$. To quantify the cloaking performance, the scattering width (SW) is determined in terms of each multipolar scattering coefficient as [16]

$$\text{SW} = \frac{4}{k_0} \sum_{n=0}^{N_{max}} (2 - \delta_{n0})|R_n|^2 \tag{14}$$

where δ_{no} is the Kronecker delta and N_{max} is the maximum relevant scattering order. Since the calculated electric sheet admittance and magnetic sheet impedance depend on the different harmonic n of scattering modes, so the scattering cancellation method can not obtain perfect cloaking. For higher scattering reduction, one should minimize the SW by minimizing the scattering coefficient of the dominant scattering mode at the operation frequency for a given object. As described in [16], when the radius of the target cylinder is electrically small (in this case, the radius of the target cylinder must be less than $0.1\lambda_0$ at the frequency of interest), only the scattering modes $n = 0$ is the dominant mode in the SW calculation. Therefore, it can be concluded that by utilizing an engineered single exclusive HMS, the SW can be significantly reduced. To obtain the optimal values of electric sheet admittance and magnetic sheet impedance to achieve invisibility, we use the diagram shown in Fig. 2, which illustrates the SW values relative to the normalized electric sheet admittance and magnetic sheet impedance variations. According to this diagram, a region with a reasonable and intelligently choice of electric sheet admittance and magnetic sheet impedance providing the smallest SW, can be considered.

As an example, let consider a PEC cylinder as a target with a radius of $b = 0.06\lambda_0$ and a dielectric spacer with relative permittivity of $\epsilon_r = 10.2$ and thickness of 1.27324 mm covered by a proper conformal HMS at 4 GHz. Figure 3 shows the SW variation versus frequency. As shown in the figure, the advantage of using HMS allows that by adjusting electric sheet admittance and magnetic sheet impedance, both the SW reduction and its corresponding bandwidth can be simultaneously adjusted. With these interpretations and with the observations of Fig. 3, it can be concluded that the use of HMS compared to the ordinary metasurfaces can have better performance in terms of SW. Figure 2 makes it possible to obtain the optimal electric sheet admittance and magnetic sheet impedance values for the design of unit cells of covering metasurface.
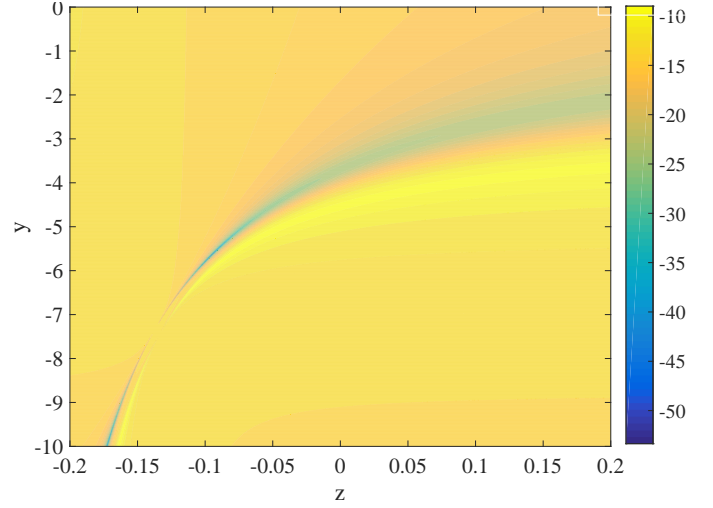

Fig. 2: SW (dB) with respect to varying $y = (j\eta_0 Y_{es})/2$ and $z = Z_{ms}/(2j\eta_0)$ corresponding to the HMS at 4 GHz.
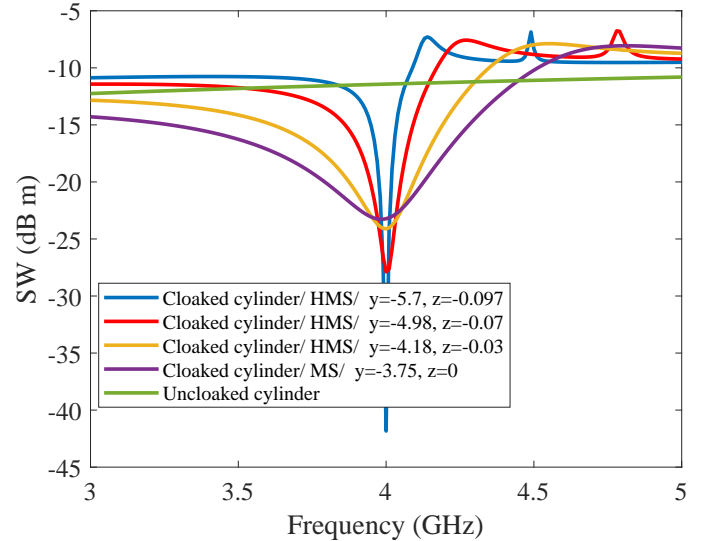

Fig. 3: SW of a PEC cylinder with a radius of $b = 0.06\lambda_0$ and a dielectric spacer with relative permittivity of $\epsilon_r = 10.2$ and thickness of 1.27324 mm covered by a proper conformal HMS.

III. Huygens' Metasurface Design

To follow the design procedures presented in Sec. II, we consider the same geometry as above. The structure of the proposed HMS to fulfill the required Y_{es} and Z_{ms} is shown in Fig. 4. It consists of a dielectric substrate with relative permittivity of $\epsilon_r = 10.2$ and the height of h, two mirror-symmetry T-shaped patches on the bottom layer to produce electric dipoles, and two mirror-symmetry split-ring resonators. A similar cell is used in [31] for spacial energy distribution manipulation application. The proposed cell can act as an HMS cell due to the simultaneous generation of induced electrical and magnetic moments. The configuration is designed for the incident plane wave shown in Fig. 1, which corresponds to the TM polarized plane wave that illuminates the considered cylinder to be cloaked. According to the equivalence principle and boundary
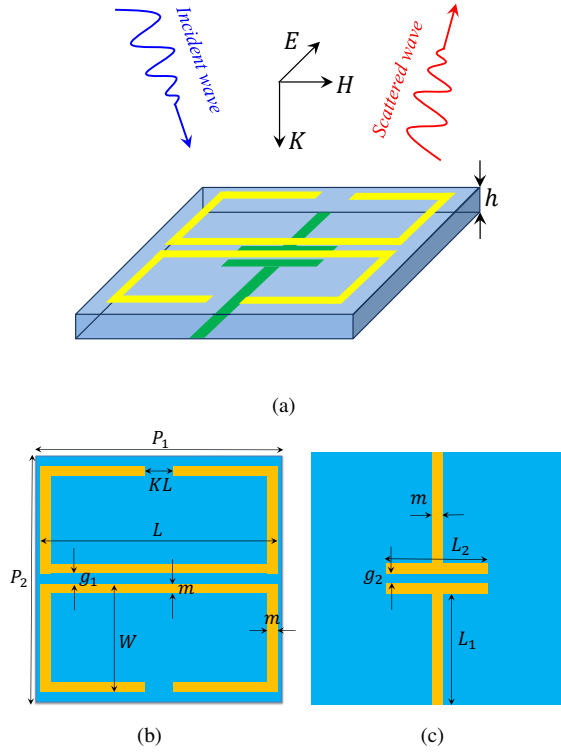
(a)

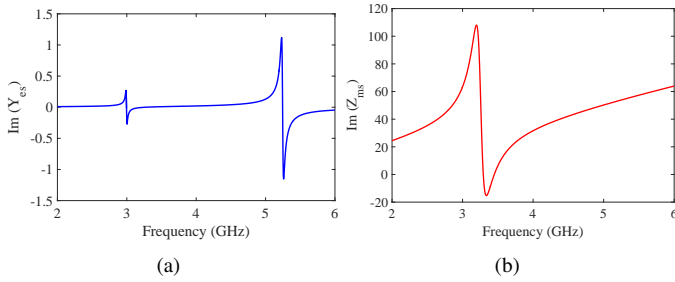Fig. 4: Geometry of the proposed planar HMS unit cell (a) 3-D view, (b) top layer, and (c) bottom layer.

Fig. 5: Simulated (a) electric sheet admittance and (b) magnetic sheet impedance.

TABLE I: Geometrical parameters of the proposed unit cell

Parameters	Values (mm)
P_1	10.78
P_2	10
h	0.5
L	9.6
L_1	4.4
L_2	4
W	4.4
g_1	0.6
g_2	0.4
m	0.4
K	0.135

conditions, the corresponding electric sheet admittance and magnetic sheet impedance can be extracted in the term of arbitrary reflection (R) and transmission (T) coefficients as [25]:

$$Y_{es} = \frac{2}{\eta_0} \frac{1 - (R+T)}{1 + (R+T)} \qquad (15)$$

$$Z_{ms} = 2\eta_0 \frac{1 + (R-T)}{1 - (R-T)} \qquad (16)$$

To calculate the electric sheet admittance and magnetic sheet impedance of the unit cell, it is truncated by periodic boundary conditions in the surrounding directions and is illuminated by a normally incident plane wave. By varying the geometric parameters of the proposed cell and optimizing its dimensions, electric sheet admittance and magnetic sheet impedance values obtained in the theory section can be tuned

using Eqs. (15) and (16) to achieve maximum invisibility. The simulated electric sheet admittance and magnetic sheet impedance corresponding to the cell are shown in Fig. 5. At the frequency of interest of 4 GHz, the simulated electric sheet admittance, and magnetic sheet impedance values are $Y_{es} = -j8.71/\eta_0$ and $Z_{ms} = j0.084\eta_0$, respectively. The optimal values of electric sheet admittance and magnetic sheet impedance extracted by full-wave simulation tools are slightly different from those obtained from the theory, but in any case, the initial cell can be designed using the values of electric sheet admittance, and magnetic sheet impedance obtained from the theory, then the dimensions of the structure can be adjusted to meet minimum SW using the proper optimization tools in CST Microwave Studio. It is worth noting that the proposed unit cell is bianisotropic, but one can demonstrate that the bianisotropy is negligible at the operating frequency range because the reflection coefficients from the two sides of the meta-atom are almost identical for a TM normal incident wave. Due to lack of space, the results of this claim and the weak bianisotropy have not been shown. The optimized geometrical parameters of the proposed HMS particle are given in Tab. I.

The reason that the proposed cell has a different resonant frequency from the designed frequency is that when used as a conformal cell for cloaking applications, a resonant frequency shift occurs and the cylinder at the frequency of 4 GHz has the maximum scattering reduction as will be shown in the next section. In fact, the goal of the planar cell simulation is to optimize its dimensions to achieve the required electric sheet admittance and magnetic sheet impedance based on the theory presented in sec. II.

IV. RESULTS AND DISCUSSION

Figure 6 shows a conducting cylinder with radius b = 5.09296 mm covered by a dielectric layer with relative permittivity of ϵ_r = 10.2 and an outer radius of a = 6.3662 mm and ultra-thin HMS with substrate relative permittivity of ϵ_r = 10.2 and thickness of h = 0.5 mm. It is illuminated by a TM^z polarized plane wave. The structure in Fig. 6 has been simulated to calculate the scattering cross section (SCS) to investigate the performance of the designed cloak. The obtained SCS reduction is close to 20 dB (suppression of 99% of the scattered wave amplitude all around the object) for normal incidence. In fact, in the analytical results, optimal values of electric sheet admittance and magnetic sheet impedance obtained from Fig. 2 are used, which are independent of the

frequency, whereas these values must be implemented with resonant meta-atoms, which are highly dispersive. It is worth noting that the analytical approach has been investigated for an infinite cylinder because of simplicity, but as in reality there is no infinite cylinder, we also obtain the scattering for the finite cylinder. In Fig. 7, the numerical result for SCS obtained with CST Microwave Studio compares to the analytical result which illustrates good agreement. The analytical SCS is extracted from the SW result using Eq. (17) [32].

$$\text{SCS} \cong \text{SW}\frac{2l^2}{\lambda} \tag{17}$$

where l is the length of the cylinder and λ is the wavelength at the operation frequency.
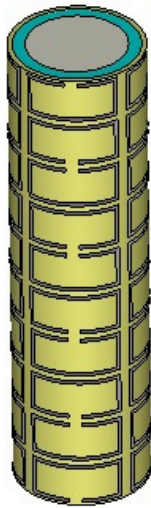

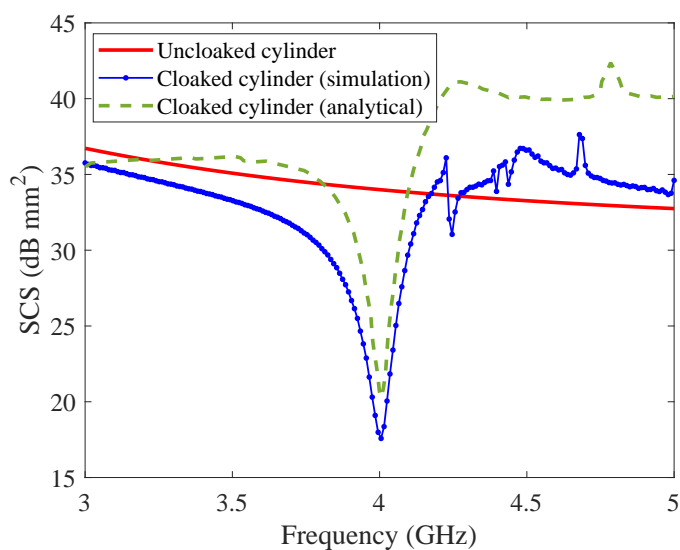Fig. 6: The conducting cylinder covered by a Huygens' metasurface.

Fig. 7: Comparison of SCS of the uncloaked and cloaked conducting cylinders.

Figure 8 depicts the corresponding total electric field distribution around uncloaked and cloaked cylinders at 4 GHz.
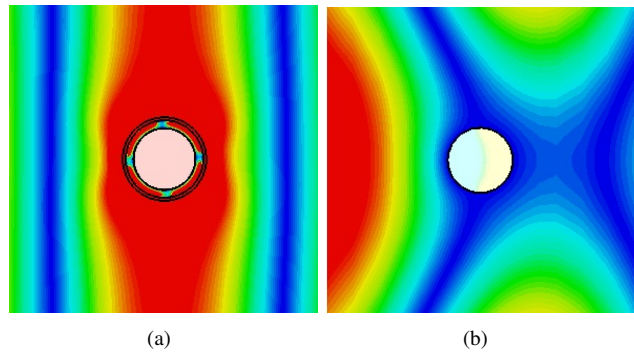

Fig. 8: Total electric field distribution around (a) cloaked and (b) uncloaked cylinders at 4 GHz.

Figure 8(a) confirms that the HMS mantle cloak significantly suppresses the scattering from the conducting cylinder restoring quasi planar field amplitudes in the near- and far-field regions, whereas as shown in Fig. 8(b) the field distribution is highly perturbed around the uncloaked cylinder. Comparing this result to the electric field distributions of cloaked cylinders in the literature such as [18], [23], [33] indicates that the designed HMS can suppress much higher scattered field than the ordinary metasurfaces. For more emphasis on better cloaking performance of HMS rather than the ordinary metasurfaces, In Fig. 9 a comparison of SCS of cloaked cylinders with an ordinary metasurface based on horizontal strips and the proposed HMS for observing θ equal to 90° versus ϕ is shown. It verifies that a higher scattering reduction is obtained by HMS. The ordinary metasurface consists of horizontal strips with optimized dimensions of the width of 7.2 mm, and periodicity of 8.3 mm, respectively. Also, the dielectric spacer has a radius equal to the outer layer of our designed HMS with a dielectric constant of $\epsilon_r = 11.5$.
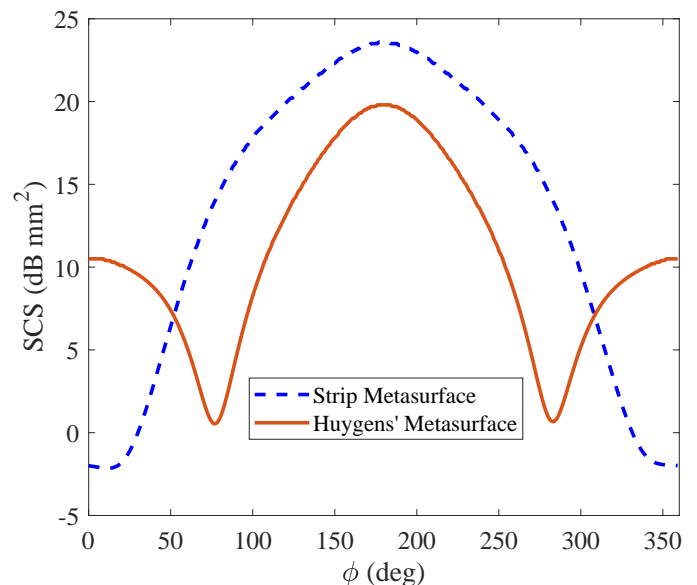

Fig. 9: Comparison of SCS of covered cylinders with strip metasurface and HMS versus ϕ.

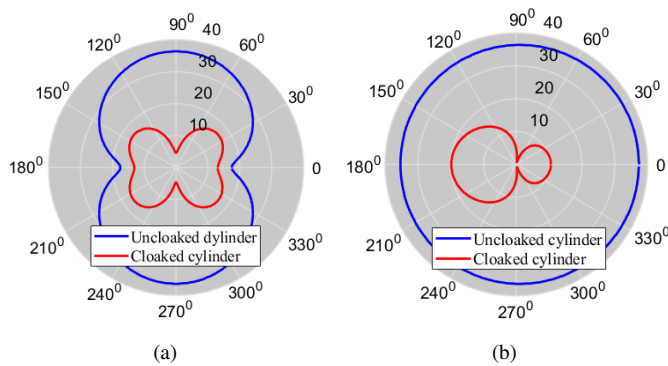Finally, Fig. 10(a) and (b) show the polar plot of SCS of

Fig. 10: SCS (dBmm^2) polar plot of cloaked and uncloaked cylinders for (a) $\phi = 90°$, and (b) $\theta = 90°$.

uncloaked and cloaked cylinders for $\phi = 90°$ and $\theta = 90°$, respectively, at the operation frequency. Remarkable scattering reduction is achieved for the cloaked cylinder in the considered two planes for all observation angles.

V. CONCLUSION

Analytical formulation to obtain required electric surface admittance and magnetic surface impedance of an HMS for cloaking purposes has been presented. The HMS has been designed to provide electric and magnetic dipoles at the operation frequency and it has been optimized to realize the required electric surface admittance and magnetic surface impedance. Simulation results illustrate remarkable scattering cancellation with HMS. Moreover, better cloaking performance of HMS rather than ordinary metasurfaces can be concluded by comparing the obtained results in this paper and presented in the literature.

REFERENCES

[1] P.-Y. Chen, F. Monticone, and A. Alu, "Suppressing the electromagnetic scattering with an helical mantle cloak," IEEE Antennas and Wireless Propagation Letters, vol. 10, pp. 1598-1601, 2011.
[2] A. Alù and N. Engheta, "Cloaked near-field scanning optical microscope tip for noninvasive near-field imaging," Physical review letters, vol. 105, no. 26, p. 263906, 2010.
[3] J. M. Lukens, D. E. Leaird, and A. M. Weiner, "A temporal cloak at telecommunication data rate," Nature, vol. 498, no. 7453, pp. 205-208, 2013.
[4] A. Alu and N. Engheta, "Plasmonic and metamaterial cloaking: physical mechanisms and potentials," Journal of Optics A: Pure and Applied Optics, vol. 10, no. 9, p. 093002, 2008.
[5] D. Ramaccia, D. L. Sounas, A. Alù, F. Bilotti, and A. Toscano, "Nonreciprocity in antenna radiation induced by space-time varying metamaterial cloaks," IEEE Antennas and Wireless Propagation Letters, vol. 17, no. 11, pp. 1968-1972, 2018.
[6] Z. J. Wong et al., "Optical and acoustic metamaterials: superlens, negative refractive index and invisibility cloak," Journal of Optics, vol. 19, no. 8, p. 084007, 2017.
[7] J. Park, J. R. Youn, and Y. S. Song, "Hydrodynamic Metamaterial Cloak for Drag-Free Flow," Physical review letters, vol. 123, no. 7, p. 074502, 2019.
[8] S. Yang, P. Liu, M. Yang, Q. Wang, J. Song, and L. Dong, "From flexible and stretchable meta-atom to metamaterial: A wearable microwave meta-skin with tunable frequency selective and cloaking effects," Scientific reports, vol. 6, p. 21921, 2016.
[9] J. C. Á. Hostos, V. D. Fachinotti, and I. Peralta, "Metamaterial for elastostatic cloaking under thermal gradients," Scientific reports, vol. 9, no. 1, pp. 1-9, 2019.
[10] K. Tsakmakidis et al., "Ultrabroadband 3D invisibility with fast-light cloaks," Nature communications, vol. 10, no. 1, pp. 1-7, 2019.
[11] J. B. Pendry, D. Schurig, and D. R. Smith, "Controlling electromagnetic fields," science, vol. 312, no. 5781, pp. 1780-1782, 2006.
[12] Y. Yang, H. Wang, F. Yu, Z. Xu, and H. Chen, "A metasurface carpet cloak for electromagnetic, acoustic and water waves," Scientific reports, vol. 6, p. 20219, 2016.
[13] M. Wei et al., "Ultrathin metasurface-based carpet cloak for terahertz wave," Optics express, vol. 25, no. 14, pp. 15635-15642, 2017.
[14] P. Alitalo, O. Luukkonen, L. Jylha, J. Venermo, and S. A. Tretyakov, "Transmission-line networks cloaking objects from electromagnetic fields," IEEE Transactions on Antennas and propagation, vol. 56, no. 2, pp. 416-424, 2008.
[15] B. Edwards, A. Alù, M. G. Silveirinha, and N. Engheta, "Experimental verification of plasmonic cloaking at microwave frequencies with metamaterials," Physical Review Letters, vol. 103, no. 15, p. 153901, 2009.
[16] A. Alù, "Mantle cloak: Invisibility induced by a surface," physical review B, vol. 80, no. 24, p. 245115, 2009.
[17] Y. Yang et al., "Full-polarization 3D metasurface cloak with preserved amplitude and phase," Advanced Materials, vol. 28, no. 32, pp. 6866-6871, 2016.
[18] Y. R. Padooru, A. B. Yakovlev, P.-Y. Chen, and A. Alù, "Analytical modeling of conformal mantle cloaks for cylindrical objects using sub-wavelength printed and slotted arrays," Journal of Applied Physics, vol. 112, no. 3, p. 034907, 2012.
[19] A. Monti, J. C. Soric, A. Alù, A. Toscano, and F. Bilotti, "Anisotropic mantle cloaks for TM and TE scattering reduction," IEEE Transactions on Antennas and Propagation, vol. 63, no. 4, pp. 1775-1788, 2015.
[20] Z. Hamzavi-Zarghani, A. Yahaghi, L. Matekovits, and A. Farmani, "Tunable mantle cloaking utilizing graphene metasurface for terahertz sensing applications," Optics Express, vol. 27, no. 24, pp. 34824-34837, 2019.
[21] V. I. Shcherbinin, Y. K. Moskvitina, V. I. Fesenko, and V. R. Tuz, "Dual-polarized all-angle cloaking of a dielectric nanowire by helical graphene ribbons," Physical Review B, vol. 100, no. 3, p. 035428, 2019.
[22] G. Moreno et al., "Wideband elliptical metasurface cloaks in printed antenna technology," IEEE Transactions on Antennas and Propagation, vol. 66, no. 7, pp. 3512-3525, 2018.
[23] C. Y. Tay, Z. N. Chen, and D. Hee, "Single-layer dual-band microwave metasurface cloak of conducting cylinder," IEEE Transactions on Antennas and Propagation, vol. 67, no. 6, pp. 4286-4290, 2019.
[24] H. Younesiraad, M. Bemani, and S. Nikmehr, "Scattering suppression and cloak for electrically large objects using cylindrical metasurface based on monolayer and multilayer mantle cloak approach," IET Microwaves, Antennas Propagation, vol. 13, no. 3, pp. 278-285, 2018.
[25] C. Pfeiffer and A. Grbic, "Metamaterial Huygens' surfaces: tailoring wave fronts with reflectionless sheets," Physical review letters, vol. 110, no. 19, p. 197401, 2013.
[26] A. M. Wong and G. V. Eleftheriades, "Perfect anomalous reflection with a bipartite Huygens' metasurface," Physical Review X, vol. 8, no. 1, p. 011036, 2018.
[27] H. Weiming, M. Deng, S. Chen, and L. Chen, "High-efficiency generation of airy beams with Huygens' metasurface." Physical Review Applied, vol. 11, no. 5, p. 054021, 2019.
[28] M. Selvanayagam and G. V. Eleftheriades, "Polarization control using tensor Huygens surfaces," IEEE Transactions on Antennas and Propagation, vol. 62, no. 12, pp. 6155-6168, 2014.
[29] M. A. Cole, D. A. Powell, and I. V. Shadrivov, "Strong terahertz absorption in all-dielectric Huygens' metasurfaces," Nanotechnology, vol. 27, no. 42, p. 424003, 2016.
[30] M. Selvanayagam and G. V. Eleftheriades, "An active electromagnetic cloak using the equivalence principle," IEEE Antennas and Wireless Propagation Letters, vol. 11, pp. 1226-1229, 2012.
[31] Zh. Wang, X, Ding, K. Zhang and Q. Wu, "Spacial energy distribution manipulation with multi-focus huygens metamirror," Scientific reports, vol. 7, pp. 1-8, 2017.
[32] A. Balanis, "Advanced Engineering Electromagnetics," Hoboken, NJ, USA: Wiley, 1989.
[33] P. Chen and et. al, "Nanostructured graphene metasurface for tunable terahertz cloaking," New Journal of Physics, vol. 15, pp. 123029-123040, 2013.